BL-6C/2015G526

Local structures in $FeSe_{1-x}Te_x$ high-temperature superconductor

Shinya HOSOKAWA,[1,*] Jens Rüdiger STELLHORN,[1] Tomohiro MATSUSHITA,[2] Naohisa HAPPO,[3] Koji KIMURA,[4] Kouichi HAYASHI,[4] and Yoshihiko TAKANO[5]
[1] Department of Physics, Kumamoto University, Kumamoto 860-8555, Japan
[2] Japan Synchrotron Radiation Research Institute (JASRI), Sayo 679-5198, Japan
[3] Graduate School of Information Sciences, Hiroshima City University, Hiroshima 731-3194, Japan
[4] Department of Physical Science and Engineering, Nagoya Institute of Technology, Nagoya 466-8555, Japan
[5] MANA, National Institute for Materials Science, Tsukuba 305-0047, Japan

Fe $K\alpha$ x-ray fluorescence holography experiments were carried out to investigate the atomic scale structure of the high-temperature superconductor $FeSe_{0.4}Te_{0.6}$. Very clear images are obtained by a sparse modeling approach to the experimental data using a L_1-regularized linear regression. The results are in good agreement with previous findings of XRD and XAFS experiments, but furthermore indicate large fluctuations in the Fe sub-lattice.

1 Introduction

By replacing Te with Se in a FeTe crystal, $FeSe_{1-x}Te_x$ shows a superconducting nature with a critical temperature of about 15 K at x = 0.4~0.5 [1], although FeTe exhibits no superconductivity. The chalcogen atoms are located at slightly different positions in a PbO-type unit cell as shown in Fig. 1. The different atomic environments of Se and Te were intensively studied by x-ray diffraction (XRD) [2], neutron diffraction (ND) [3], and x-ray absorption fine structure (XAFS) [4].

Based on an *ab initio* structure optimization of the structures, a direct influence of the displacements of Se and Te on the hybridization of the Fe orbitals and the charge distribution was found [3,5], which can lead to magnetic instabilities in the material.

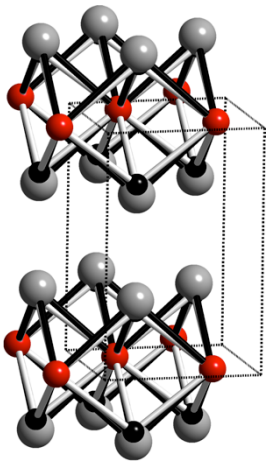

Fig. 1: Layer structure in the $FeSe_{0.4}Te_{0.6}$ tetragonal crystal [2,3]. Large-, medium- and small-sized balls indicate Te, Fe and Se atoms, respectively. Taken from Ref. [7].

Thus, the local structure is a key point to understand the superconducting properties of $FeSe_{1-x}Te_x$. A newly developed technique for atom-resolved characterizations of the local structure of materials is x-ray fluorescence holography (XFH) [6], which can provide three-dimensional (3D) atomic images around a specific element emitting fluorescent x-rays. Compared with other experimental methods, no specific model of the atomic structure is necessary. In this work, we will present Fe $K\alpha$ XFH measurements on the $FeSe_{0.4}Te_{0.6}$ superconductor [7].

2 Experiment

A single crystal of $FeSe_{0.4}Te_{0.6}$ was grown using a slow-cooling method from the melt. In the slow-cooling method, a polycrystal raw sample was placed in a BN crucible sealed in an Ar-filled Mo capsule. It was then heated to 1150°C, followed by cooling to 780°C for 80 h, and then cooled to room temperature. The crystal was cleaved with a flat (001) surface larger of about 3 × 3 mm^2.

The XFH technique is based on the angular dependence of the x-ray fluorescence intensity from an emitter atom caused by an interference of an incident x-ray wave with the waves scattered from nearby atoms. The Fe $K\alpha$ (6.403 keV) XFH measurements were carried out at BL-6C of PF-KEK and at BL39XU of SPring-8. For this experiment, the holograms were measured in the azimuthal angular range of $0° \le \phi \le 360°$ in steps of ~0.35° and in the incident angular range of $0° \le \theta \le 75°$ in steps of 1°. They were expanded using the fourfold rotational symmetry along the [001] axis and the three mirror symmetries of the (100), (010), and (001) planes. The sample was cooled to 100 K by a liquid N_2 cryo-stream.

The XFH measurements were performed at eight different incident energies between 7.5 and 11.0 keV in steps of 0.5 keV. Further details on the XFH method and its implementation can be found elsewhere [6]. The recorded holograms were used to reconstruct the local atomic environment around the Fe atoms in real space by a scattering pattern matrix extraction algorithm using L_1

regularized linear regression (SPEA-L1) [8] representing a sparse modeling approach to the experimental data.

3 Results and Discussion

The hologram measured at 9.0 keV is exemplary displayed in Fig. 2(a) in an orthographic projection, in comparison with a hologram by computer simulation in (b). The color scale indicates the variation of the fluorescence intensity relative to the averaged value. The hologram is centered at $\theta = 0^{\circ}$, and the radial and angular direction indicate θ and ϕ, respectively. The magnitudes of the experimental and theoretical holograms are mostly the same values of ± 0.4%, while the features of the holograms are different from each other, indicating that the real atomic configurations around the Fe atoms would be different from the ideal ones, such as positional fluctuations.

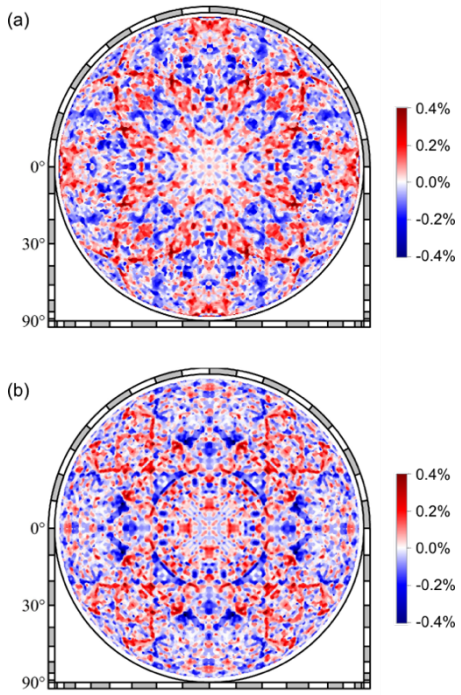

Fig. 2: Orthographic projection of (a) the hologram measured at 9.0 keV in comparison with (b) that by computer simulation. The magnitude of the holographic oscillations is given as a color bar. Taken from Ref. [7].

The real-space reconstructions of the (010) and (001) planes in $FeSe_{1-x}Te_x$ are illustrated in Figs. 3(a) and (b), respectively. The Fe emitter atoms are located at the center of the figures. The magnitudes of the images are normalized to that of the nearest neighboring atoms on the (010) plane. The intensity scale is given as a color bar beside the images, ranging between 0.1 and 1.0, i.e. the lower 10% of the image intensity is regarded as the experimental noise level and not displayed here.

The reconstruction on the (010) plane in Fig. 3(a) shows the layer of the Fe atoms along the x axis, and the layer of the first Se/Te neighbors as indicated with the dotted lines. Note that there are two orientations of the tetrahedral, i.e. a half of the Fe atoms have chalcogen neighbors on the positive z-side, and a half have those on the negative z-side, which are superimposed in this figure. The peak of the chalcogen signal is located at a 'height' (z component of the coordinate) of 0.17 nm, with a slight shoulder near 0.15 nm, which are in good agreement with the chalcogen heights reported by XRD (0.1478 nm for Se and 0.1718 nm for Te [2]) and by XAFS investigations (0.147 nm for Se and 0.175 nm for Te [4]) for the similar $FeSe_{1-x}Te_x$ compounds. The intensity difference reflects the atomic numbers of Se and Te and their concentration ratio.

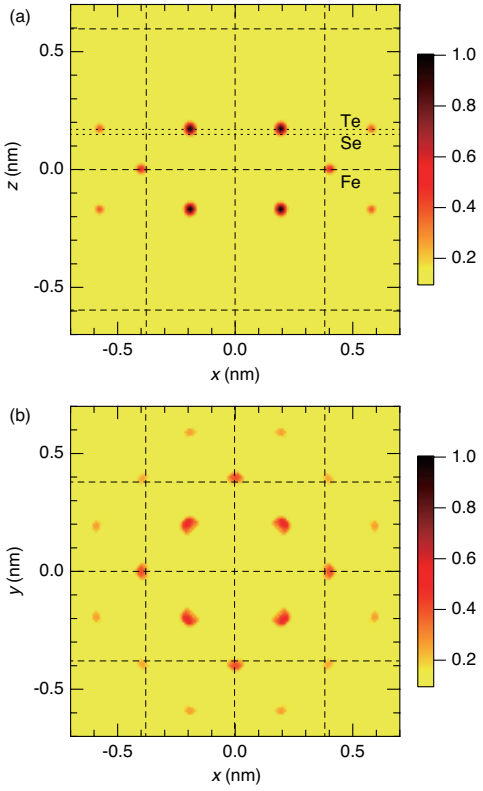

Fig. 3: Reconstructions on (a) the (010) plane and (b) the (001) plane in $FeSe_{0.4}Te_{0.6}$ from the experimental holograms by SPEA-L1. The dashed lines indicate the unit cell, and the dotted lines in (a) indicate the expected heights of the chalcogen atoms. Images are scaled with respect to the strongest signal in (a) as given by the color bars. Taken from Ref. [7].

The face-centered Fe sub-lattice of on the (001) plane is clearly visible in Fig. 3(b). Signals can be observed up to the 4th Fe neighboring atoms. The sub-lattice is much clearer and contains mostly no artificial signals as was in the previous reconstructions [9], which may be attributed to the improved reconstruction algorithm and to the lower sample temperature. The images of Fe are, nevertheless, comparatively weak and widely spread. We interpret this as a sign for large positional fluctuations of the neighboring Fe atoms.

In summary, Fe $K\alpha$ XFH experiments were carried out

to investigate the atomic scale structure of the high-temperature superconductor $FeSe_{0.4}Te_{0.6}$. Very clear images are obtained by a sparse modeling approach to the experimental data using a L_1-regularized linear regression. The results are in good agreement with previous findings of XRD and XAFS experiments, but furthermore indicate large fluctuations in the Fe sub-lattice.

Acknowledgement

The XFH experiments were performed at BL-6C of KEK-PF (No. 2015G526) and at BL39XU at SPring-8 (Nos: 2014B1187, 2015B1183, 2016A1136). This work was supported by the Japan Society for the Promotion of Science (JSPS) Grant-in-Aid for Scientific Research on Innovative Areas '3D Active-Site Science' (No. 26105006, 26105013) and 'Sparse Modeling' (No. 16H01553). JRS gratefully acknowledges financial support as Overseas Researcher under the Postdoctoral Fellowship of JSPS (No. P16796).

References

[1] K.-W. Yeh, T.-W. Huang, Y.-L. Huang, T.-K. Chen, F.-C. Hsu, P. M. Wu, Y.-C. Lee, Y.-Y. Chu, C.-L. Chen, and J.-Y. Luo, *Europhys. Lett.* **84**, 37002 (2008).

[2] M. Tegel, C. Löhnert, and D. Johrendt, *Solid State Commun*. **150**, 383 (2010).

[3] D. Louca, K. Horigane, A. Llobet, R. Arita, S. Ji, N. Katayama, S. Konbu, K. Nakamura, T.-Y. Koo, P. Tong, and K. Yamada, *Phys. Rev B* **81**, 134524 (2010).

[4] B. Joseph, A. Iadecola, A. Puri, L. Simonelli, Y. Mizuguchi, Y. Takano, and N. L. Saini, *Phys. Rev B* **82**, 020502(R) (2010).

[5] C.-Y. Moon and H. J. Choi, *Phys. Rev. Lett.* **104**, 057003 (2010).

[6] K. Hayashi, N. Happo, S. Hosokawa, W. Hu, and T. Matsushita, *J. Phys.: Condens. Matter* **24**, 093201 (2012).

[7] J. R. Stellhorn, Y. Ideguchi, K. Kimura, K. Hayashi, N. Happo, M. Suzuki, H. Okazaki, A. Yamashita, Y. Takano, and S. Hosokawa, *Phys. Stat. Sol. B*, in press.

[8] T. Matsushita, *e-J. Surf. Sci. Nanotech.* **14**, 158 (2016).

[9] Y. Ideguchi, K. Kamimura, K. Kimura, S. Hosokawa, N. Happo, K. Hayashi, Y. Ebisu, T. Ozaki, J. R. Stellhorn, M. Suzuki, H. Okazaki, A. Yamashita, and Y. Takano, *Z. Phys. Chem.* **230**, 489 (2016).

* shhosokawa@kumamoto-u.ac.jp